2020 IEEE/ASME International Conference on
Advanced Intelligent Mechatronics (AIM), Boston, USA
(Virtual Conference), July 6-9, 2020

Analysis and Control of a Body-Attached Spring-Mass Runner Based on Central Pivot Point Approach

O. Kaan Karagoz[†*], Izel Sever[†*], Uluc Saranli[‡], and M. Mert Ankarali[†]

***Abstract*— The Spring-Loaded Inverted Pendulum (SLIP) template and its extensions have long been used as benchmark models for analyzing the dynamics of legged systems in biology and robotics. The fundamental SLIP model is composed of single point mass attached to the ground (during stance phase) via an ideal lossless spring. Many researchers introduced various extensions to this fundamental model, such as damping & torque actuation, to handle critical physical phenomena that are unavoidable in real systems. Another crucial missing concept in SLIP template is the effect of the upper body in humans and humanoid robotic systems on the closed-loop system dynamics. Even though the SLIP template can effectively capture COM behavior, it cannot provide a framework for describing full-body stabilization and control. In this paper, we present a new control policy called the Central Pivot Point (CPP) for the body attached spring-mass runners. In the stance phase, CPP directs ground reaction forces through the center of mass and cancels the torque created by these forces on the body. In this way, the CPP model makes it possible to develop different controllers for both the body's rotational and euclidean dynamics. Firstly, we analyze the characteristics and stability of the periodic solutions of the CPP model. Then, we develop a PD controller for pitch dynamics and an LQR (Linear Quadratic Regulator) for gait level apex to apex discrete dynamics to stabilize the system's periodic solutions. We compute the basin of attraction of the proposed control scheme and show examples of how the model behaves under disturbances. The results show that the purposed model and associated control policy could be beneficial in the design and control of humanoid robotic systems.**

I. INTRODUCTION

The superior mobility of legged animals compared to other terrestrial platforms is accompanied by dynamics that include non-linear, complex, and hybrid elements [1]–[3]. To overcome these difficulties while designing a legged robotic system or explaining animal locomotion, Full and Koditschek proposed a hierarchical structure [4]. In this framework, while simple yet effective models that are called "templates" explain targeted behavior such as running & walking, parsimonious models that are called "anchor" account for real or more complex systems. Creating or finding policies on anchor models, such that anchor behaves like a template establishes the connection between a template and an anchor. This structure enables the use of simpler models to analyze & control legged robots or explain animal behavior [5]–[9].

Spring-loaded inverted pendulum (SLIP) model is one of the most well-known, widely used templates to explain and use as a control target for running behavior [10], [11]. Although the SLIP model can define the behavior of COM dynamics adequately, it does not provide a framework on how to stabilize the upper body dynamics, which is probably very critical to be neglected in humans and humanoid systems. Several studies introduced methods such as reactive PD (Proportional, Derivative) controller [8], passive geometric stability [12], and gyro-stabilizer [13] in order to keep the upper body in balance during stable legged locomotion. However, when such methods are in action, it becomes difficult to track the center of mass trajectories defined by the SLIP model [14]. For this reason, instead of SLIP, more inclusive templates that include upper body dynamics may be a better choice in terms of descriptive accuracy as well as robustness and efficiency of locomotion.

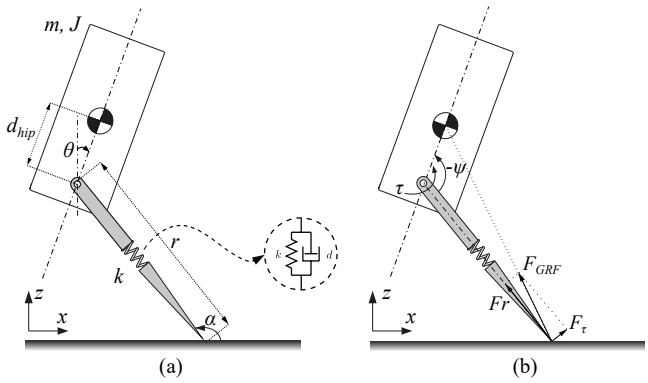


Fig. 1. The Trunk-Spring Loaded Inverted Pendulum (T-SLIP) model. **a)** Physical parameters, **b)** Central Pivot Point model and forces and torques acting on the model.

Poulakakis and Grizzle introduced the first template model, Asymmetric SLIP[1](ASLIP), that integrates the upper body dynamics into a SLIP like model [15]. Then, they proposed a hierarchical control structure that can potentially both stabilize the body dynamics as well as the locomotion. At the first level, they apply a continuous control policy at the stance phase to maintain the body around the desired posture and create an invariant manifold on which SLIP like dynamics can be applied. At the second level, they used a gait level SLIP based controller to regulate the locomotion.

Later, Maus et al. [18] introduced the Virtual Pivot Point concept using the same template model in [15], inspired

The authors are with the Department of Electrical and Electronics Engineering[†] and the Department of Computer Engineering[‡], Middle East Technical University, 06800 Ankara, Turkey. *I. Sever and O. K. Karagoz contributed equally to this work. {izel.sever, karagoz.osman, mertan}@metu.edu.tr[†] {saranli}@ceng.metu.edu.tr[‡]

[1]This template is called Asymmetric SLIP (ASLIP) in [16], Trunk-SLIP (TSLIP) in [17]. We refer this template as TSLIP throughout this dissertation.

978-1-7281-6794-7/20/$31.00 ©2020 IEEE

Authorized licensed use limited to: ULAKBIM UASL - MIDDLE EAST TECHNICAL UNIVERSITY. Downloaded on March 25,2021 at 09:55:20 UTC from IEEE Xplore. Restrictions apply.

by the experimental locomotion data of human, dog, and chicken. This model expresses running behavior, aiming to stabilize the body like a virtual stable pendulum employing a spring located between the hip and the foot and a virtual pivot point created above the center of mass.

In this study, we have developed and examined the stability of a new control policy, which we call the Central Pivot Point (CPP), for the body attached spring-mass runner. CPP, in the stance phase, directs ground reaction forces through the center of mass and cancels the torque created by these forces on the body of the template model represented in Fig. 1(a). In this way, the CPP model makes it possible to develop different controllers for both the body's rotational and euclidean dynamics.

In addition, the existence and analysis of the periodic solutions of such systems are vital as it allows them to be controlled with the least possible effort (such as energy, torque) without opposing the conditions dictated by the natural dynamics of the system. At the same time, it makes it possible to develop controllers on these trajectories, since the presence of periodic solutions brings a mathematical explanation to the system's trajectories. Therefore, we systematically investigated the existence and characteristics of the periodic solutions of the CPP controlled model in this paper. Then, we stabilize the periodic solutions of the CPP by developing a PD controller for the pitch dynamics and LQR (Linear Quadratic Regulator) for euclidean dynamics. We compute the basin of attraction of the proposed control scheme and show examples of how the model behaves under disturbances.

The organization of the paper is as follows: Section II represents the TSLIP template, CPP concept, necessary tools to analyze such systems, and the gait controller to stabilize the model. Section III reports the periodic solutions of the CPP concept, periodic solution's dependence on control parameters of the model, the stability of periodic solutions, and how the model performs under the gait controller.

II. CENTRAL PIVOT POINT CONCEPT

A. Trunk-SLIP Model

Trunk-SLIP (TSLIP) model, first presented in [16], is a more comprehensive model for physical systems that have non-trivial upper body dynamics. TSLIP has a hip joint that does not coincide with the center of mass (COM) of the body with mass m and inertia J, see Fig. 1(a). The model has a mass-less leg that includes a spring, k, and active damping, d. The only actuation of the model is the torque at the hip joint. Table I presents the definitions of the variables and parameters for the model given in Fig. 1. The values of the physical parameters in Table I are adopted from [17].

TSLIP model has two phases, flight, and stance. In both phases, the model has 3 degrees of freedom and $q = [x,\ z,\ \theta]^T$ defines the generalized coordinates of the model. While, in the flight phase, the center of mass follows a ballistic trajectory which is defined by

$$\ddot{\mathbf{q}} \;=\; \begin{bmatrix} 0 \\ -g \\ 0 \end{bmatrix}, \tag{1}$$

in the stance phase, the dynamics take the form

$$\ddot{\mathbf{q}} = \begin{bmatrix} 1/m & 0 & 0 \\ 0 & 1/m & 0 \\ 0 & 0 & 1/J \end{bmatrix} \left(D_q\psi\ \tau + D_q r\ F_r - \begin{bmatrix} 0 \\ mg \\ 0 \end{bmatrix} \right), \tag{2}$$

where F_r, τ, ψ are leg force, hip torque and body-leg angle, respectively (see Fig. 1(b) and Table I). In (2), $D_q\psi$ and $D_q r$ stand for Jacobian (column) matrices whose elements are the derivatives of ψ and r with respect to state variables, q, respectively. Also, eqn. (2) results in non-integrable stance dynamics similar to the basic SLIP model [19].

The leg force is given by $F_r = -k(r - r_0) - d\dot{r}$. The damping coefficient, d, is set by the controller to a fixed value before the start of the stance-phase. Nominal value (when the system is on the desired periodic solution) of the damping value is 0, and we tune d to stabilize and control the fixed points.

TABLE I
PARAMETERS AND THEIR DEFINITIONS

Physical Parameters	**Symbol**	**Value (unit)**
Mass of the body	m	80 (kg)
Moment of inertia of the body	J	5 $(kg.m^2)$
Leg rest length	r_0	1 (m)
Distance between the hip and the COM	d_{hip}	0.1 (m)
Spring coefficient	k	20 (kN/m)
Control Parameters	**Symbol**	**(Unit)**
Touchdown angle	α	(deg)
Active damping	d	$(N.s/m)$
Proportional gain	K_p	-
Derivative gain	K_d	-

B. Central Pivot Point Concept

The main idea behind the CPP concept is that it applies torque from the hip to prevent the formation of any torque on the body. The hip torque, which makes the CPP available by directing the ground reaction forces to the COM throughout the whole movement in the stance, is calculated as a function of F_r as

$$\tau_m = F_r\ r\ \frac{d_{hip}\ sin(\psi)}{r - d_{hip}\ cos(\psi)}\ . \tag{3}$$

Under the effect of τ_m, the pitch dynamics of the TSLIP model are separated from the other dynamics. In this way, we can apply separate controllers to stabilize the system.

C. Model Analysis

Poincaré Map Method is a useful tool to analyze the running behavior because of its non-linear, complex, and periodic nature. This method intersects the periodic trajectories of a system whose state-space model is defined by n generalized coordinates with a hyper-plane so that the flow of the periodic system is expressed independently in time with

Authorized licensed use limited to: ULAKBIM UASL - MIDDLE EAST TECHNICAL UNIVERSITY. Downloaded on March 25,2021 at 09:55:20 UTC from IEEE Xplore. Restrictions apply.

$n-1$ coordinates. This hyper-plane crossing the trajectories is called the Poincaré Section. If the k^{th} intersection of the system state vector with this hyper-plane is called $\mathbf{X}_k$, the relationship between the two consecutive intersections can be expressed by defining the Poincaré Map as $F(\mathbf{X}_k) = \mathbf{X}_{k+1}$.

The periodic solutions of a system are the trajectories that always intersect the Poincaré Section from the same point, that is, $F(\mathbf{X}^*) = \mathbf{X}^*$. This point, $\mathbf{X}^*$, on the Poincaré Section is called a fixed point. It is possible to comment on the local stability of a system by computing the Jacobian matrix of the Poincaré Map on the fixed points.

In the CPP Model, the hyper-plane specified by $\dot{z} = 0$ and $\ddot{z} < 0$ conditions can be selected as the Poincaré Section. These conditions define the highest position of the system on the vertical axis in the flight phase. Since the position of the system on the horizontal axis in the flight phase, x does not affect dynamics, on this hyper-plane, the system status vector is defined $\mathbf{X}_k = [z,\ \dot{x},\ \theta,\ \dot{\theta}]^T$ with four coordinates. However, $\dot{\theta} = 0$ is required for the existence of any fixed point. Therefore, the fixed point subspace is in 3 dimensional space, $\mathbf{X}_k^s = [z,\ \dot{x},\ \theta,\ 0]^T$.

The local stability of the fixed points can be analyzed by computing eigenvalues of the Jacobian matrix, $A = \frac{\partial P}{\partial \mathbf{X}}(\mathbf{X}^*)$. If the maximum eigenvalue of A is less than 1, the model is stable.

D. The Gait Controller

Since τ_m separates the pitch dynamics and euclidean dynamics, we can develop a separate controller for both dynamics. For pitch dynamics we form a PD law with high gain in the form of $\tau_{pd} = (K_p(\theta^* - \theta) - K_d\dot{\theta})$. The resulting hip torque becomes

$$\tau = \tau_m + \tau_{pd}\ . \tag{4}$$

If the pitch angle is at a desired orientation, all ground reaction forces pass through the COM. Otherwise, PD law tries to rotate the body to the desired orientation.

To stabilize other degrees of freedom (z and $\dot{x}$), we developed an event-based controller using LQR [20] and we chose the leg angle at touchdown, α_{td}, and damping ratio, d, as controller parameters. α_{td} is well known widely used control input for the SLIP model [21]–[23] and damping controller is effectively used in a hopper to inject energy into the system or remove energy from the system [24]. In the flight phase, LQR calculates the necessary α_{td} and d to stabilize the model.

With these control inputs, the Poincaré Map becomes $F(\mathbf{X}_k, \mathbf{u}_k) = \mathbf{X}_{k+1}$ where $\mathbf{u}_k = [\alpha_{td},\ d]^T$. The linearization of F around $\mathbf{X}_k$ yields

$$\Delta\mathbf{X}_{k+1} = A\Delta\mathbf{X}_k + B\Delta\mathbf{u}_k\ . \tag{5}$$

where $\Delta\mathbf{X}_k = \mathbf{X}_k - \mathbf{X}^*$, $\Delta\mathbf{u}_k = \mathbf{u}_k - \mathbf{u}^*$ and $B = \frac{\partial P}{\partial \mathbf{X}}(\mathbf{u}^*)$. We assume that high gain PD law fixes the error in θ and $\dot{\theta}$. We do not consider the effect of the pitch dynamics to z and $\dot{x}$, and we do not try to stabilize pitch dynamics using LQR. Hence, we use the sub-matrices of A and B which correspond to Δz and $\Delta\dot{x}$ while constructing LQR problem. Let us define $A[1,2;1,2]$ is [2x2] matrix obtained from the first two columns and the first two rows of A, let $B[1,2;1,2]$ is [2x2] matrix obtained from the first two columns and the first two rows of B, then $A_S = A[1,2;1,2]$ and $B_S = B[1,2;1,2]$ are the matrices that we are interested in.

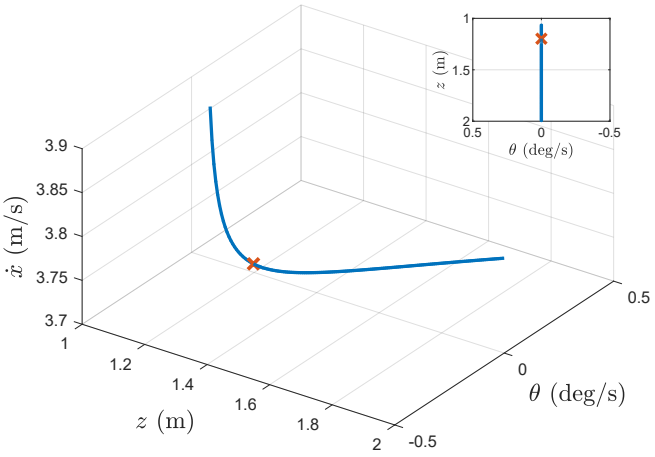


Fig. 2. The fixed point distribution of CPP model when $\alpha_{td} = 109.8°$. The red "x" represents the fixed point $\mathbf{X}^* = [1.2,\ 3.7096,\ 0,\ 0]^T$.

The cost function of infinite-horizon LQR controller as follows

$$J = \sum_{k=1}^{\infty} \mathbf{X}_k^T Q \mathbf{X}_k\ , \tag{6}$$

where Q is a positive definite matrix. Since CPP is a conceptual model, we only consider state weights, we do not include inputs to the J. We construct the optimal state feedback, K, by

$$K = (B_S^T P B_S)^{-1} B_S^T P A_S\ , \tag{7}$$

where P is the solution of the following discrete Riccati Algebraic Equation

$$P = Q + A_S^T (P - P B_S (B_S^T P B_S)^{-1} B_S^T P) A_S\ . \tag{8}$$

Finally, $\mathbf{u}_k$ in Eq. (5) is calculated as follows

$$\mathbf{u}_k = -\begin{pmatrix} K \\ 0 \end{pmatrix} \Delta\mathbf{X}_k\ . \tag{9}$$

III. RESULTS

A. The Fixed Points of CPP Concept

As we stated in Section II-A, there is no analytic solution of (2). We have to use numerical analysis methods to find the fixed point subspace of the CPP. We integrate the dynamics of the model using MATLAB "ode45" from apex to apex to compute Poincaré Map, F. Because of the errors come from numerical integration and round-off, finding the fixed points of the model becomes a search problem such that identifying the set $S_{\mathbf{X}^*} := \{\mathbf{X}_k^s \mid M > \|\mathbf{X}_k^s - \mathbf{X}_{k+1}^s\|\}$ gives the subspace of the fixed points, for a given M which is the threshold that determines which apex states are a fixed point. The numerical integration tolerance, the optimization

Authorized licensed use limited to: ULAKBIM UASL - MIDDLE EAST TECHNICAL UNIVERSITY. Downloaded on March 25,2021 at 09:55:20 UTC from IEEE Xplore. Restrictions apply.

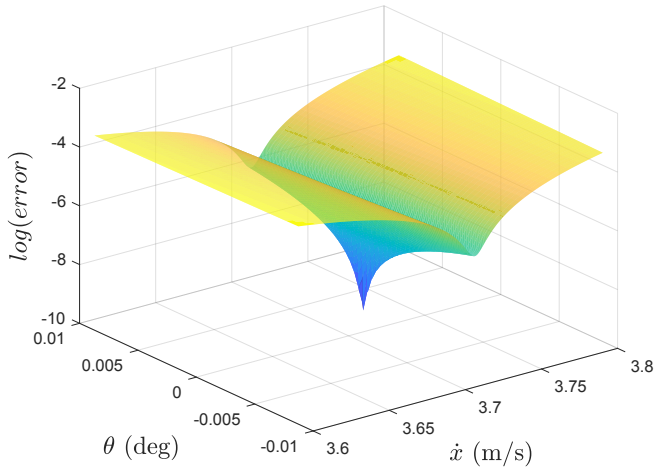


Fig. 3. Evaluation of $\|\mathbf{X}_k^s - \mathbf{X}_{k+1}^s\|$ on $z = 1.2m$

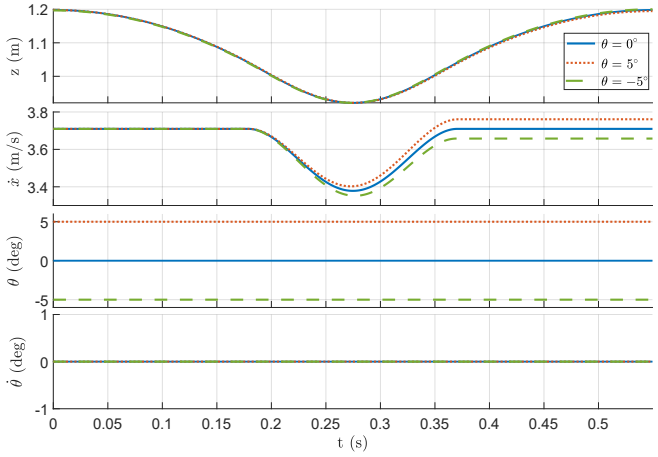


Fig. 4. Change of apex state in one step for $\theta = 0°$, $\theta = 5°$ and $\theta = -5°$.

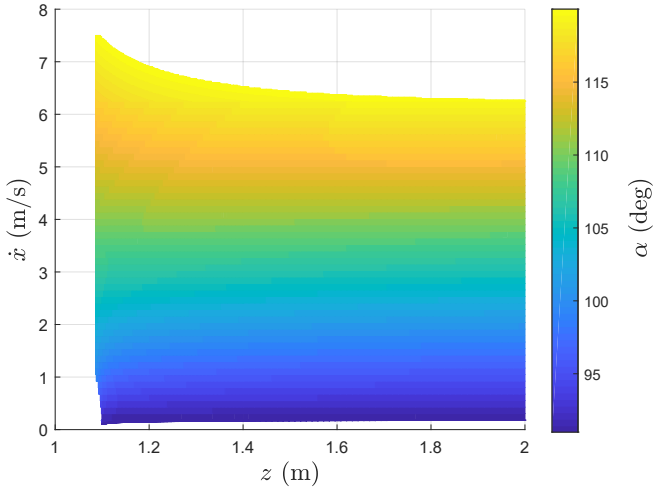


Fig. 5. Variation of the fixed point subspace by the leg angle at touchdown, α_{td}.

algorithm tolerance, and M should be compatible with each other.

To specify the set $S_{\mathbf{X}^*}$, we initialized "fminunc" algorithm of MATLAB from many different starting points that scan three-dimensional space, $\mathbf{X}_k^s = [z,\ \dot{x},\ \theta,\ 0]^T$. "fminunc" algorithm minimizes the function $\underset{\mathbf{X}_k^s}{\operatorname{argmin}} \|\mathbf{X}_k^s - \mathbf{X}_{k+1}^s\|$ for each point. If a point that is found by "fminunc" algorithm satisfies the constraint $M > \|\mathbf{X}_k^s - \mathbf{X}_{k+1}^s\|$, it becomes an element of the set $S_{\mathbf{X}^*}$.

Since we look for the fixed points of the CPP model all the control parameters should be at their nominal value, $d = 0$, $K_p = 0$ and $K_d = 0$, and we selected $\alpha_{td} = 109.8°$ for this example. For a given M, the resulting $S_{\mathbf{X}^*}$ is a curve on the plane that is defined by $\theta = 0°$, see Fig. 2. This shows that the fixed point subspace is one-dimensional and lies on the plane defined by $\theta = 0°$ for $\alpha_{td} = 109.8°$.

To strengthen our claim we chose the plane defined by $z = 1.2m$ which intersects the curve in Fig. 2 at the point which is shown by red "x" and we evaluated $error = \|\mathbf{X}_k^s - \mathbf{X}_{k+1}^s\|$ all over the plane and the resulting $error$ can be seen on Fig. 3. As expected, we have a single minimum on this plane, which is the point of intersection of the fixed point subspace and $z = 1.2m$ plane. Thus, we can conclude that our claim is true for $\alpha_{td} = 109.8°$. By making the same simulations, we validated that the claim holds for $91° < \alpha_{td} < 120°$.

We give an example of how the states of a fixed point evolve from apex to apex on Fig. 4. We started the simulation from $\mathbf{X}^* = [1.2,\ 3.7096,\ 0,\ 0]^T$ which is shown by the red "x" in Fig. 2 and plotted its states in Fig. 4. As expected, all the states returned their starting locations. Since all ground reaction forces pass through the center of mass, $\ddot{\theta}$ is 0, consequently $\dot{\theta}$ and θ are conserved.

Also, we investigated the apex states that are not on $\theta = 0°$ in Fig. 4. When the body leans forward, the system gains energy by increasing its speed at the apex state while conserving its height. On the other hand, it loses its energy when the body leans backward. These results also show why the fixed point subspace is located on $\theta = 0°$.

Additionally, we looked for the fixed points for different α_{td}. We carried out the fixed point search on this interval: $0.8 < z < 2$, $0 < \dot{x} < 7.5$, $\theta = 0°$ and $\dot{\theta} = 0°$. Fig. 5 represents the distribution of fixed points depending on α_{td}. A given α_{td} almost all heights, z, the fixed points exist. Along with the change in α_{td}, it is observed that the curve of fixed point space shifts in the direction of $\dot{x}$. This shows that we can cover a large portion of $(z, \dot{x})$ space by changing α.

We evaluated the stability of the fixed points on Fig. 5. The results are on Fig. 6. As seen, there exists a small stable region of fixed points on the upper left corner. However, most of them are unstable; hence a controller is needed to stabilize the system and to create a basin of attraction for a desired fixed point.

B. Stability Analysis and Basins of Attraction of the Gait Controller

After investigating the fixed point existence of the system, we implemented the high gain PD controller to control the

Authorized licensed use limited to: ULAKBIM UASL - MIDDLE EAST TECHNICAL UNIVERSITY. Downloaded on March 25,2021 at 09:55:20 UTC from IEEE Xplore. Restrictions apply.

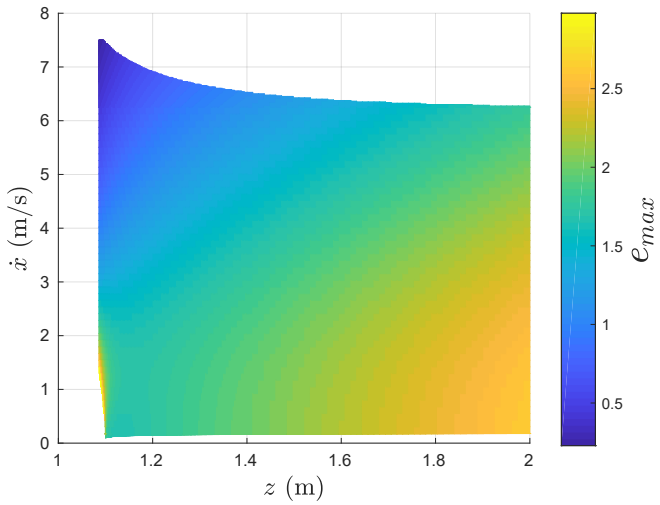


Fig. 6. Maximum eigenvalues, e_{max} of the Jacobi matrix calculated by using the fixed points given in Fig. 5.

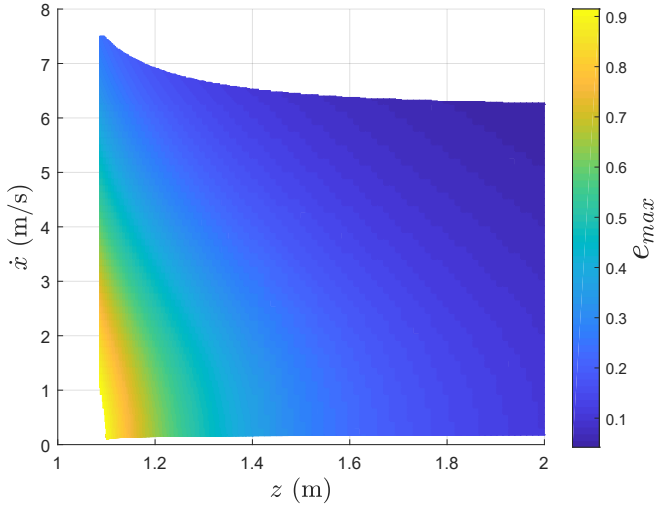


Fig. 7. Maximum eigenvalues, e_{max} of the Jacobi matrix calculated by using the fixed points obtained when the system runs under the action of the controller.

pitch dynamics and the LQR controller to regulate the height and the forward velocity by actively stabilizing the running behavior. As stated earlier, the stability characteristics of the system with no controller is given in Fig. 5, and only a small portion of the eigenvalues are less than one, meaning that the most of the fixed points are unstable. As shown in Fig. 6, all the eigenvalues can be made less than one by using the PD controller and LQR to achieve a stable gait. Moreover, as seen in the example run in Fig. 8, the control structure leads to a stable periodic solution. In this running experiment, initial condition is given as $\mathbf{X}_0 = [2m, 4m/s, 20°, 100°/s]^T$. Fig. 8 indicates that the gait of the model converges to a periodic solution with minimal steady-state error (less than 1%), indicating that the combination of the PD controller with the LQR controller accomplishes the stability of locomotion in approximately less than ten steps.

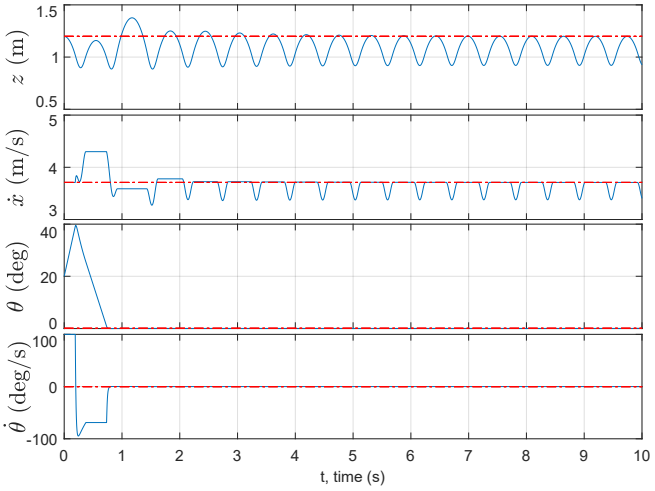


Fig. 8. The height, z, COM forward velocity,$\dot{x}$, pitch angle, θ and pitch rate $\dot{\theta}$ of the system with an example running simulation with an initial point of $z = 1.9m$, $\dot{x} = 4m/s$, $\theta = 20°$, $\dot{\theta} = 100°/s$, aiming to reach the fixed point state $\mathbf{X}^* = [1.2,\ 3.7096,\ 0,\ 0]^T$.The dashed red lines show the desired nominal values which is the fixed point values.

We conducted simulations to characterize the basins of attraction of our model and to define the stability properties of the gait controller. In these simulations, we operated the system by providing different initial conditions and checked whether it converged to a pre-determined fixed point, precisely $\mathbf{X}^* = [1.2m,\ 3.7096m/s,\ 0°,\ 0°/s]^T$. We considered the gait is stable if the system ran for 30 seconds, and the deviation from the fixed point at the last apex state was less than 1% of the fixed point.

In the Fig. 9, the variation in the stable basin of attraction of the system for different initial conditions is given. First, we analyzed the domain of attraction by keeping the pitch angle and the pitch rate as zero and sweeping the initial speed and height in an extensive range. Then investigate the behavior of the system by applying pitch angle $\theta = 20°$ and pitch rate $\dot{\theta} = 100°/s$, separately. The shaded green region in Fig. 9, shifted in the direction of increasing $\dot{x}$ while the shaded area remains almost the same if we add disturbance on pitch angle or the pitch rate. There is no torque limitation; therefore, stable locomotion can be attained with our controller even when we initiated the system at radical disturbances.

IV. CONCLUSIONS

In this paper, we presented a new method named Central Pivot Point (CPP) for controlling the TSLIP model, which includes pitch dynamics. We systematically analyzed the fixed points of the system and showed that the majority of the fixed points of the model are unstable. Using the fact that CPP separates the pitch dynamics and euclidean dynamics, we developed a high gain PD controller for pitch dynamics and an LQR for euclidean dynamics. We showed that the purposed controller structure could stabilize all the fixed points of the model. Also, we tested the performance of the gait controller under disturbances. We illustrated the existence and stability of periodic solutions with a large

Authorized licensed use limited to: ULAKBIM UASL - MIDDLE EAST TECHNICAL UNIVERSITY. Downloaded on March 25,2021 at 09:55:20 UTC from IEEE Xplore. Restrictions apply.

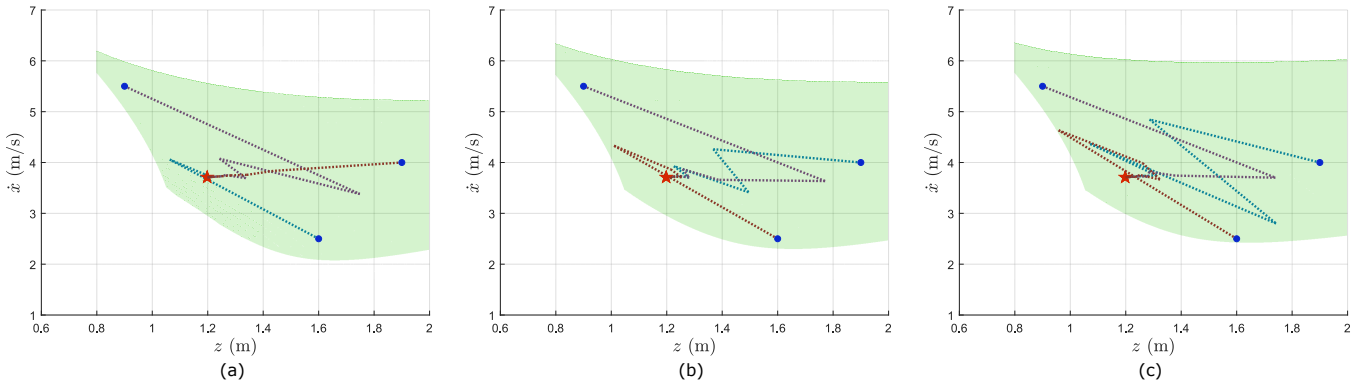


Fig. 9. This figure illustrates the stable domain of attraction for the system under the gait level LQR controller. The green region implies the initial apex-state conditions from which the system converges to a stable fixed point which is $z^* = 1.2m$ and $\dot{x}^* = 3.7096m/s$. The dashed lines stand for example simulations which show that the progression of the apex states. Simulations are conducted with **a)** $\theta = 0°$, $\dot{\theta} = 0°/s$ **b)** $\theta = 20°$, $\dot{\theta} = 0°/s$ **c)** $\theta = 0°$, $\dot{\theta} = 100°/s$.

domain of attraction through many simulation experiments and showed that our control structure could reject even radical disturbances in states. In this work, we show the effectiveness and robustness of the gait controller on the TSLIP template.

In the future, we intend to obtain analytic approximations to the ground reaction forces and the stance trajectories of the TSLIP model and attain SLIP fit to these approximations. We plan to use the CPP as a control target for humanoid systems in a simulation environment.

ACKNOWLEDGMENT

This work was supported by The Scientific and Technological Research Council of Turkey (TUBITAK) through Project 117E106, I. Sever's, and O. K. Karagoz's scholarships.

REFERENCES

[1] T. Kubow and R. Full, "The role of the mechanical system in control: a hypothesis of self–stabilization in hexapedal runners," *Philosophical Transactions of the Royal Society of London. Series B: Biological Sciences*, vol. 354, no. 1385, pp. 849–861, 1999.

[2] M. H. Dickinson, C. T. Farley, R. J. Full, M. Koehl, R. Kram, and S. Lehman, "How animals move: an integrative view," *science*, vol. 288, no. 5463, pp. 100–106, 2000.

[3] C. Li, T. Zhang, and D. I. Goldman, "A terradynamics of legged locomotion on granular media," *science*, vol. 339, no. 6126, pp. 1408–1412, 2013.

[4] R. J. Full and D. E. Koditschek, "Templates and anchors: neuromechanical hypotheses of legged locomotion on land," *Journal of experimental biology*, vol. 202, no. 23, pp. 3325–3332, 1999.

[5] M. Ahmadi and M. Buehler, "The arl monopod ii running robot: Control and energetics," in *Proceedings 1999 IEEE International Conference on Robotics and Automation (Cat. No. 99CH36288C)*, vol. 3. IEEE, 1999, pp. 1689–1694.

[6] A. Hereid, S. Kolathaya, M. S. Jones, J. Van Why, J. W. Hurst, and A. D. Ames, "Dynamic multi-domain bipedal walking with atrias through slip based human-inspired control," in *Proceedings of the 17th international conference on Hybrid systems: computation and control*. ACM, 2014, pp. 263–272.

[7] U. Saranli and D. E. Koditschek, "Template based control of hexapedal running," in *2003 IEEE International Conference on Robotics and Automation (Cat. No. 03CH37422)*, vol. 1. IEEE, 2003, pp. 1374–1379.

[8] M. M. Ankaralı and U. Saranlı, "Control of underactuated planar pronking through an embedded spring-mass hopper template," *Autonomous Robots*, vol. 30, no. 2, pp. 217–231, 2011.

[9] W.-C. Lu, M.-Y. Yu, and P.-C. Lin, "Clock-torqued rolling slip model and its application to variable-speed running in a hexapod robot," *IEEE Transactions on Robotics*, vol. 34, no. 6, pp. 1643–1650, 2018.

[10] W. J. Schwind, "Spring loaded inverted pendulum running: A plant model." Ph.D. dissertation, 1998.

[11] P. Holmes, R. J. Full, D. Koditschek, and J. Guckenheimer, "The dynamics of legged locomotion: Models, analyses, and challenges," *SIAM review*, vol. 48, no. 2, pp. 207–304, 2006.

[12] B. Brown and G. Zeglin, "The bow leg hopping robot," in *Proceedings. 1998 IEEE International Conference on Robotics and Automation (Cat. No. 98CH36146)*, vol. 1. IEEE, 1998, pp. 781–786.

[13] N. Shemer and A. Degani, "Analytical control parameters of the swing leg retraction method using an instantaneous slip model," in *2014 IEEE/RSJ International Conference on Intelligent Robots and Systems*. IEEE, 2014, pp. 4065–4070.

[14] W. C. Martin, A. Wu, and H. Geyer, "Experimental evaluation of deadbeat running on the atrias biped," *IEEE Robotics and Automation Letters*, vol. 2, no. 2, pp. 1085–1092, 2017.

[15] I. Poulakakis and J. W. Grizzle, "The spring loaded inverted pendulum as the hybrid zero dynamics of an asymmetric hopper," *IEEE Transactions on Automatic Control*, vol. 54, no. 8, pp. 1779–1793, 2009.

[16] I. Poulakakis and J. Grizzle, "Formal embedding of the spring loaded inverted pendulum in an asymmetric hopper," in *2007 European Control Conference (ECC)*. IEEE, 2007, pp. 3159–3166.

[17] M. A. Sharbafi, C. Maufroy, M. N. Ahmadabadi, M. J. Yazdanpanah, and A. Seyfarth, "Robust hopping based on virtual pendulum posture control," *Bioinspiration & biomimetics*, vol. 8, no. 3, p. 036002, 2013.

[18] H.-M. Maus, S. Lipfert, M. Gross, J. Rummel, and A. Seyfarth, "Upright human gait did not provide a major mechanical challenge for our ancestors," *Nature communications*, vol. 1, p. 70, 2010.

[19] P. Holmes, "Poincaré, celestial mechanics, dynamical-systems theory and "chaos"," *Physics Reports*, vol. 193, no. 3, pp. 137–163, 1990.

[20] G. C. Goodwin, S. F. Graebe, M. E. Salgado, *et al.*, *Control system design*. Upper Saddle River, NJ: Prentice Hall,, 2001.

[21] Ö. Arslan and U. Saranli, "Reactive planning and control of planar spring–mass running on rough terrain," *IEEE Transactions on Robotics*, vol. 28, no. 3, pp. 567–579, 2012.

[22] T. Cnops, Z. Gan, and C. D. Remy, "The basin of attraction for running robots: Fractals, multistep trajectories, and the choice of control," in *2015 IEEE/RSJ International Conference on Intelligent Robots and Systems (IROS)*. IEEE, 2015, pp. 1586–1591.

[23] R. M. Ghigliazza, R. Altendorfer, P. Holmes, and D. Koditschek, "A simply stabilized running model," *SIAM review*, vol. 47, no. 3, pp. 519–549, 2005.

[24] G. Secer and U. Saranli, "Control of planar spring–mass running through virtual tuning of radial leg damping," *IEEE Transactions on Robotics*, no. 99, pp. 1–14, 2018.

Authorized licensed use limited to: ULAKBIM UASL - MIDDLE EAST TECHNICAL UNIVERSITY. Downloaded on March 25,2021 at 09:55:20 UTC from IEEE Xplore. Restrictions apply.